BioMetals 1996, 9, 57–65

The application of laser microprobe mass analysis to the study of biological material

Theodore C. Iancu*, Daniel P. Perl†, Irmin Sternlieb¶, Aaron Lerner*, Esther Leshinsky‡, Edwin H. Kolodny‡, Amy Hsu† & Paul F. Good†

**Pediatric Research Unit, Carmel Hospital and B. Rappaport Faculty of Medicine, Technion-Israel Institute of Technology, Haifa, Israel, † the Arthur M. Fishberg Research Center for Neurobiology, Mount Sinai Medical Center, New York, NY, ¶ the National Center for the Study of Wilson's Disease, New York, NY, and ‡ the Department of Neurology, New York University School of Medicine, New York, NY, USA*

Received 9 May 1995; accepted for publication 19 May 1995

Laser microprobe mass analysis (LAMMA) is an investigational method which is a powerful tool for the identification and quantitation of various elements present in small volumes of tissue. LAMMA is highly sensitive and capable of rapidly detecting concentrations of 1–3 p.p.m. of most metallic elements, in precisely localized cellular compartments. In order to further assess its value, cultured skin fibroblasts and biopsy tissues from human subjects and experimental animals were probed by LAMMA, and the results were correlated with ultrastructural findings. Biopsy samples were obtained from patients suffering from Gaucher disease, and from patients and animals with pathologic iron or copper metabolism. No significant abnormalities were detected in the cultured fibroblasts from patients with Gaucher disease, in contrast to the iron content of tissue biopsy Gaucher cells, which was markedly increased, apparently as a consequence of erythrophagocytosis. Particularly intense iron-related peaks were found in liver cytosiderosis due to neonatal or genetic haemochromatosis, thalassaemia major and in animal models of iron overload. An additional finding was the presence of aluminium accumulation in siderosomes of different cells. In liver biopsy samples from human Wilson's disease and from rats with an inherited disorder causing copper toxicosis, copper-containing compounds were identified and localized, and their relative concentration was estimated by LAMMA. The present study showed that LAMMA is a valuable technique for the localization and estimation of relative abundance of trace elements in various tissues containing excessive amounts of metals.

Keywords: aluminium, copper, electron microscopy, Gaucher disease, iron, laser microprobe mass spectrometry

Introduction

In recent years, analytic techniques have become available for the identification and localization of specific elements in tissues, some with the capability of elemental quantitation within subcellular structures. Secondary mass spectrometry (SIMS), which is highly sensitive having a minimum detection limit of 1 p.p.m. or better, has the capability of providing maps of specific elemental distribution. Its major drawback is the lack of histological identification of analysed structures and the fact that the primary ion beam target interaction is a surface phenomenon with virtually no penetration of the sample (Perl & Good 1992). By contrast, laser microprobe mass analysis (LAMMA), initially developed in Germany about 20 years ago (Hillenkamp *et al.* 1974), provides similar sensitivity to SIMS, with the clear advantage of precise histological localization of the studied element at the cellular level. Yet this technique has seen relatively limited use with biological materials (Schmidt *et al.* 1980, Verbeuken *et al.* 1988) even though it enables histological localization and identification of probe sites in plastic-embedded tissues with resultant quantitation at a minimum detection limit of 5 p.p.m. for most elements (Good *et al.* 1992a,b). To further assess the role of LAMMA as a refinement in the cellular localization of metals in certain pathological conditions, we used LAMMA and transmission electron microscopy (TEM) on the same samples of cultured fibroblasts and on tissue samples from patients with storage diseases and from animal models of human diseases.

Address for correspondence: T. C. Iancu, Electron Microscopy Laboratories, B. Rappaport Faculty of Medicine, PO Box 9649, Haifa 31096, Israel. Fax: (+972)4-8517008.

Materials and methods

Fibroblast cultures

Fibroblasts were cultured from skin explants of patients with Gaucher disease (type I, non-neuronopathic). After obtaining informed consent, punch biopsies of forearm skin were taken from patients suspected (and subsequently confirmed) to have this condition. Control fibroblasts (line GM00043 A) were obtained from the Human Genetic Mutant Cell Repository (Cornell Institute for Medical Research, Camden, NJ), and grown in Dulbecco's modified Eagle's medium with 15% fetal calf serum and penicillin–streptomycin–glutamine. A pellet of confluent cells, harvested by trypsinization, was suspended in 1% agar, fixed in 4% paraformaldehyde and processed by routine procedures for electron microscopy and LAMMA. For each sample of cultured fibroblasts, at least four grids were cut from three different blocks.

Liver biopsy specimens

These were taken from patients with Gaucher disease, neonatal haemochromatosis, genetic haemochromatosis, thalassaemia major and Wilson's disease in whom the final diagnosis was confirmed by additional investigations. All biopsies had been obtained for earlier diagnostic studies, none being performed for the LAMMA study itself.

Iron overload: spontaneous conditions

Tissue samples from homozygous hypotransferrinaemic mutant mice (*hpx/hpx*) aged 2 and 12 months were obtained from Dr R. J. Simpson (Department of Clinical Biochemistry, King's College School of Medicine and Dentistry, London, UK). Their biochemical, histopathological and ultrastructural abnormalities have been previously reported (Simpson *et al.* 1991, Iancu *et al.* 1995). The liver of captive exotic birds had been studied earlier by light and electron microscopy (Ward *et al.* 1988), and part of the same material was used for the present study.

Parenteral iron overload

Brissot *et al.* (1983) injected intramuscular iron sorbitol or iron polymaltose into baboons (*Papio papio*) for 15 months (3–5 days each week, total amount 20–26 g iron). Liver biopsy specimens were also studied by electron microscopy (Iancu *et al.* 1985) and samples obtained at the end of the overload period were used for the LAMMA study.

Copper metabolism

Long–Evans–Cinnamon (LEC) rats, an inbred strain of mutant rats, develop a hereditary hepatitis with high liver copper concentrations, low serum ceruloplasmin and copper levels, and morphologic abnormalities of liver cells similar to those of human Wilson's disease (Li *et al.* 1991). Recently they have been demonstrated to have a deletion in the copper transporting gene homologous to the Wilson disease gene (Wu *et al.* 1994). We examined liver tissue from two LEC rats, made available by The National Center for the Study of Wilson's Disease, New York.

Electron microscopy

The various tissue samples were fixed in 3% glutaraldehyde in 0.1 M cacodylate buffer (pH 7.4) for 2 h, postfixed in 1% osmium tetroxide for 1 h, dehydrated in graded ethanol or acetone series, and embedded in either Spurr's resin or epoxy. For identification and localization of ferritin and haemosiderin, ultrathin sections were either left unstained or stained with lead citrate for 2 min, and then viewed and photographed through JEOL JEM 100B and 100CX electron microscopes at 80 kV.

LAMMA

The LAMMA 500 instrument (Leybold-Heracus, Cologne, Germany) combines a high-resolution optical microscope with a time-of-flight mass spectrometer. The instrument is equipped with a high-power pulsed neodymium-YAG laser that is focused through a Zeiss Ultrafluar glycerin immersion objective (×100) also used for visualization of the specimen. To target the point of interest, the LAMMA uses the collinear continuous low-energy He:Ne laser, seen as a red spot on the section. After selection of the area to be probed, the high power laser pulse is triggered, producing a perforation of the specimen measuring 1–2 μm in diameter. From this perforation in the section, positively (or in an alternative mode, negatively) charged ions produced by vaporization and ionization of the tissue are separated by acceleration within an ion lens and detected according to their time-of-flight along a 1.8 m long vacuum column. Each perforation in the tissue specimen provides multielement detection at the part per million level, displayed immediately on the screen of the attached computer system which stores the data for further analysis (Good *et al.* 1992a,b).

In the present study we used semi-thin (0.75 μm thick) sections of plastic-embedded tissue specimens, prepared in parallel with the samples for electron microscopic examination. Toluidine blue stained sections were mounted on standard 3 mm diameter electron microscopy grids and placed in vacuum behind a quartz cover slip inserted in a movable (x–y axis) specimen holder. The following subcellular compartments were probed: (1) cytoplasmic *granules* (presumably secondary lysosomes) when present as distinct organelles in the cytosol and resolvable by light microscopy; (2) *cytosol*, in areas where no lysosome-like organelles were visible; and (3) *nuclei*. In addition, intracellular accumulations, such as glycogen and fat droplets in hepatocytes, were also probed and usually served as a control for an adjacent cellular compartment. When appropriate, bile contents in dilated canaliculi, acellular amorphous material in liver sinusoids, collagen bundles and interstitial stroma, or erythrocytes in liver sinusoids, were probed for comparison with the other target sites.

Results

General considerations

The assessment of the contribution of LAMMA in identifying and localizing various elements in biological specimens was obtained by comparing spectra obtained from abnormal areas with those obtained from uninvolved tissue compartments or from control specimens, and by correlating the findings with information gained from biochemical, histochemical and electron microscopic findings from the same specimens.

Cultured skin fibroblasts

Laser microprobe mass analysis of cultured skin fibroblasts from patients with Gaucher disease did not demonstrate significant abnormalities in any of the samples studied. Electron microscopy did not show any ultrastructural changes in the cultured fibroblasts of patients with this condition.

Tissue samples

Gaucher cells, liver. LAMMA revealed prominent iron-related peaks (mass to charge ratio, $m/z = 56$) from probe sites which were unevenly distributed in these cells. The dense cytoplasmic compartment generated high peaks (Figure 1a), with much lower peaks in the pale, glucocerebroside-containing tubular structures of the 'Gaucher bdies' (Table 1). By TEM it was shown that the cytoplasmic iron-related peaks are generated by abundant typical ferritin particles. Occasional membrane-limited organelles containing iron-rich ferritin particles (siderosomes) were also seen.

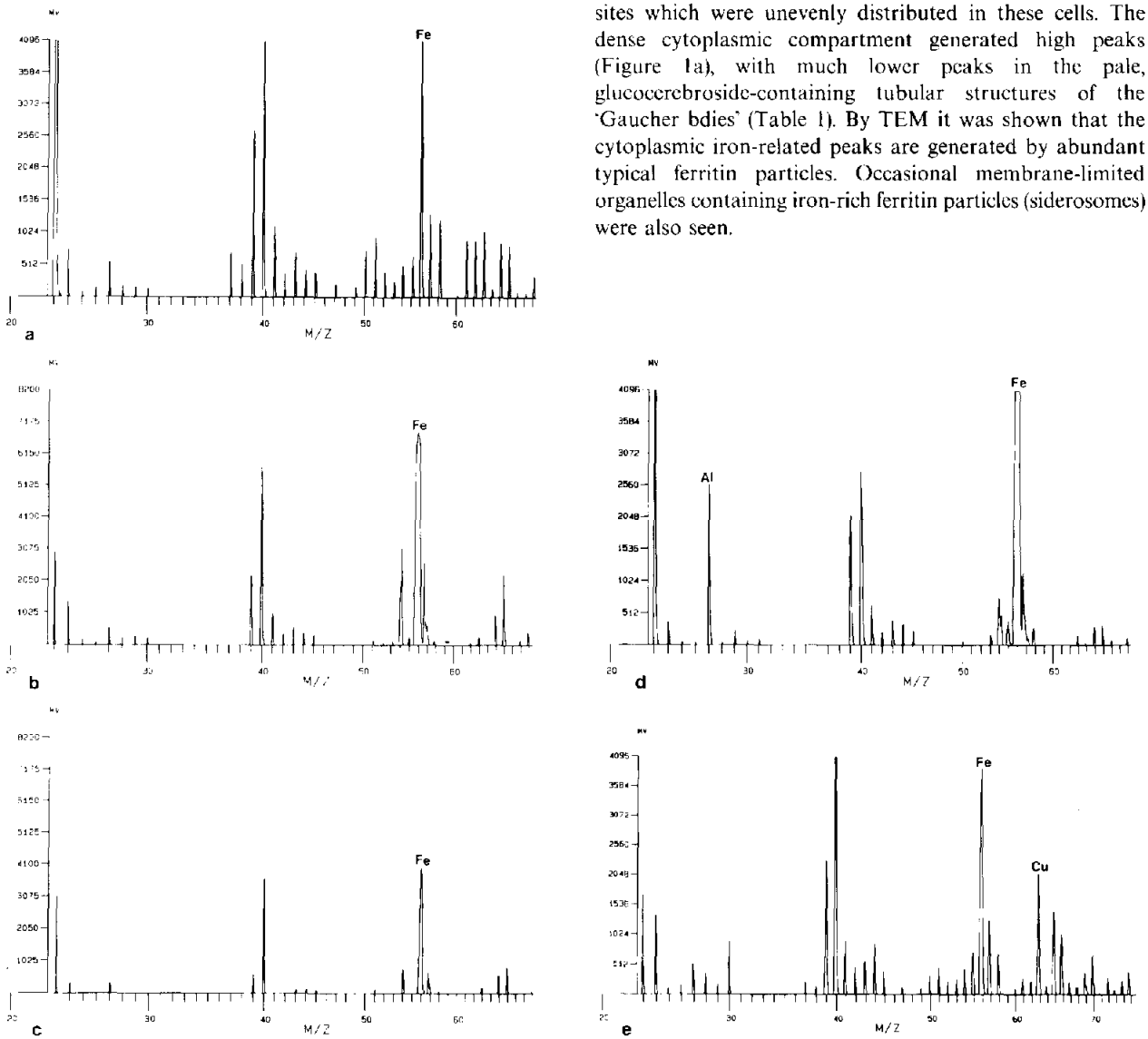

Figure 1. Partial mass spectra from various samples probed by LAMMA. Positive ion spectra show major peaks identified by their mass to charge ratios (m/z) where they are assumed to have a unit positive charge. Ordinate gives peak height rather than integrated peak intensity. Na 23; Mg 24; Al 27; P 30; S 32; K 39; Ca 40; Fe 56; Cu 63. (**a**) Cytoplasm of a Gaucher cell showing a high iron-related peak ($m/z = 56$). (**b**) Genetic haemochromatosis, prior to phlebotomics; siderosomes in hepatocytes. (**c**) Same sample as (**b**), but the probed cell was a Kupffer cell; note that the iron-related peak is much lower than that of hepatocytic siderosomes. (**d**) Thalassaemia major, liver biopsy of a 3 month old infant showing an extremely high iron signal (saturated peak), as well as a significant aluminium peak ($m/z = 27$). (**e**) Wilson's disease, patient 1. Probing of connective tissue cells from the pre-transplant cirrhotic liver show prominent copper ($m/z = 63$) and iron ($m/z = 56$) peaks.

Table 1. LAMMA probing of tissue samples from patients with Gaucher disease

Sample and compartment	Mass spectrum intensity (V)	
	Fe ($m/z = 56$)	Cu ($m/z = 63$)
Gaucher cells, tubular structures	10 ± 4	15 ± 5
Gaucher cells, cytosol	116 ± 113	25 ± 6
Gaucher cells, nuclei	4 ± 1	23 ± 6
Hepatocyte cytosol	3 ± 1	20 ± 4
Hepatocyte nuclei	3 ± 1	26 ± 2

The data represent mean of three samples each. For each compartment examined, 20–80 probe sites were collected, for this and Tables 2 and 3. Signals are expressed as the mean integrated peak intensity ± SEM.

Neonatal haemochromatosis. As expected, LAMMA showed very prominent iron-related peaks ($m/z = 56$) in both the cytosolic and siderosomic compartment of hepatocytes (Table 2). The iron-related peaks obtained when probing the sinusoidal cells were not equally prominent and were seen to originate mainly from isolated siderosomes. TEM, like light microscopy, confirmed the reported disarray and damage to liver cells in this disease (Knisely 1992). Hepatocytes showed marked siderosis, evident as conspicuous ferritin particles randomly dispersed in the cytosol, but also as siderosomes loaded either with iron-rich ferritin particles or haemosiderin (Figure 2).

Genetic haemochromatosis. LAMMA showed prominent iron-related ($m/z = 56$) peaks in cytosol and siderosomes of hepatocytes, with relative sparing of sinusoidal cells (Figures 1b and c, and Table 2). Patients undergoing phlebotomy until in negative iron balance, showed no prominent iron-related peaks in specimens obtained from follow-up biopsies.

Thalassaemia major. LAMMA identified increased iron in the cytosolic compartment (seen as ferritin by TEM) as well as conspicuous accumulation of iron in hepatocytic siderosomes in a liver biopsy specimen of a 3 month old infant, confirming our earlier observations (Iancu *et al.* 1977, Iancu 1983) (Figure 1d and Table 2). Even at this early age and before transfusional therapy, some iron deposition was noticeable in the siderosomes of sinusoidal cells, by both LAMMA (Table 2). In later stages of thalassaemia major (5 year old), the overload of sinusoidal cells was more conspicuous, while the parenchymal load appeared to have reached a plateau.

Mutant hpx/hpx *hypotransferrinaemic mice.* These mice develop an early, diffuse iron accumulation in hepatocytes, pancreatic acinar cells, heart and small intestinal myocytes, with remarkable sparing of the liver reticuloendothelial system (RES) and of splenic cells (Simpson *et al.* 1993). The LAMMA study confirmed these and the TEM findings (Iancu *et al.* 1995). In 12 month old mice the iron overload was more generalized, involving the RES cells as well.

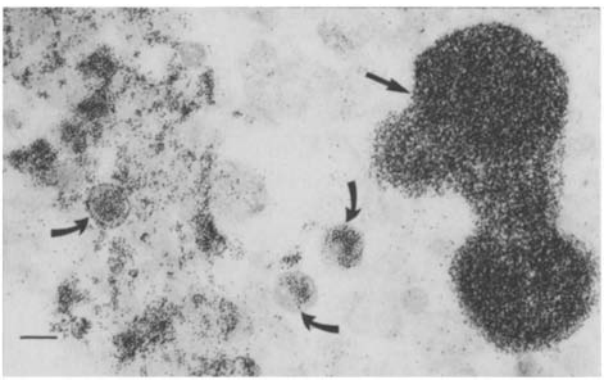

Figure 2. Neonatal haemochromatosis. In this condition, ferritin and haemosiderin are found in extremely large amounts in hepatocytes both in the cytosol and siderosomes. This electron micrograph shows a haemosiderin-containing siderosome (arrow) and other membrane-bound bodies filled with iron-rich ferritin particles (curved arrows). When probed by LAMMA, these iron aggregates generate very high mass 56 peaks. Unstained. Bar: 100 nm.

LAMMA differentiated iron accumulation between the cytosolic and lysosomal compartments of iron-loaded cells by detection of much higher iron-related peaks in siderosomes. Prominent aluminium-related peaks ($m/z = 27$) were also encountered in the probed siderosomes (Table 2). LAMMA also showed that the electron-dense material visible within the bile canaliculi of older animals contained large amounts of iron and aluminium.

Captive exotic birds. Many exotic birds kept in aviaries develop severe iron overload of the liver parenchymal cells and RES (Ward *et al.* 1988). LAMMA showed that the highest iron-related peaks were obtained from the massive hemosiderin aggregates in both cell types which characterize the light and electron microscopic findings in these birds. Significant aluminium-related peaks ($m/z = 27$) were also seen in spectra taken from dense siderosomes of hepatocytes and sinusoidal cells (Table 2).

Baboons. LAMMA showed iron-related peaks in the cytosol and especially in siderosomes of hepatocytes from baboons injected with iron sorbitol or iron polymaltose for up to 15 months (Iancu *et al.* 1985). Aggregates located in sinusoidal cells, also generated high iron-related peaks. The aluminium-related peaks, although prominent, did not reach the level observed in the siderosomes of the hornbill (Table 2).

Wilson's disease. LAMMA studies of liver biopsy specimens from Wilson's disease showed an increased copper content ($m/z = 63$) in all three studied patients, even though not to the same degree in all cell types (Table 3). Tissue from patient 1 was from a pre-transplant specimen of a markedly cirrhotic liver, with the highest copper-related signal in cells from the fibrotic tissue and other non-parenchymal cells. This specimen also showed prominent iron-related peaks.

Table 2. Tissue iron concentration and LAMMA data in iron overload

Sample and compartment	Iron concentration (μmol g^{-1} dry tissue)	Mass spectrum intensity (V)		
		Al ($m/z=27$)	Fe ($m/z=56$)	Cu ($m/z=63$)
Hornbill, liver	830			
hepatocytes				
cytosol		9±2	123±28	5±1
siderosomes		144±20	865±83	1±0.5
nuclei		15±4	69±12	10±2
sinusoidal cells		141±15	766±31	0.5±0.2
sinusoidal erythrocytes		14±4	44±6	15±2
Baboon, liver	1050±750			
hepatocytes				
cytosol		8±1	154±22	21±2
siderosomes		37±6	1193±112	2±1
nuclei		8±3	53±19	21±2
sinusoidal cells		40±5	1115±16	n.a.
Hypotransferrinemic mice (12 months)	47±6			
hepatocytes				
cytosol		7±2	150±24	19±2
siderosomes		29±6	383±45	15±2
nuclei		5±1	31±4	31±3
bile canaliculi		28±5	370±15	14±2
sinusoidal cells		14±2	322±50	12±2
Neonatal haemochromatosis	318			
hepatocytes				
cytosol		6±1	62±6	31±3
siderosomes		44±5	547±209	21±2
nuclei		8±1	59±6	45±4
sinusoidal cells		24±5	354±65	24±4
Genetic haemochromatosis	365			
hepatocytes				
cytosol		0.8±0.2	41±11	12±1
siderosomes		19±4	622±81	15±1
nuclei		2±0.3	2±1	14±1
sinusoidal cells		8±3	278±38	18±2
Thalassaemia major (3 months)	330			
hepatocytes				
cytosol		19±4	400±55	11±3
siderosomes		31±5	320±32	29±3
nuclei		4±1	22±4	19±3
sinusoidal cells		9±3	208±28	15±3.3
Thalassaemia major (5 years)	620			
hepatocytes				
cytosol		5.0±1	32±5	15±1
siderosomes		13±4	773±71	4±2
nuclei		2±0.7	9±2	14±1
sinusoidal cells		12±2	473±70	8±2

(Figure 1e). High copper and iron peaks were also detected in the hepatocytic nuclei of this specimen. Patients 2 and 3 were twin brothers aged 10 years with Wilson's disease and advanced liver disease. Patient 2 had prominent copper-related peaks in all probed compartments, while his brother, patient 3, had much lower signals, possibly related to the fact that the biopsy was performed after 2 months of chelating therapy (Table 3).

LEC rats. Prominent copper and iron peaks were found by LAMMA in sinusoidal cells and in the nuclei of hepatocytes of both rats examined. Rat 2 had also prominent iron peaks in the hepatocytic cytosol (Table 3). TEM of unstained ultrathin sections showed conspicuous ferritin in the cytosol, and ferritin and haemosiderin in the siderosomes of sinusoidal cells, which were found to have high iron peaks by LAMMA (Figure 3).

Table 3. Tissue copper concentrations and LAMMA data in conditions with abnormal copper metabolism

Sample and compartment		Mass spectrum intensity (V)		
		Al ($m/z=27$)	Fe ($m/z=56$)	Cu ($m/z=63$)
Control liver biopsy[a]				
hepatocytes				
cytosolic granules[b]		3.2±0.7	2.7±0.3	10±2.2
nuclei		0.1±0.1	0.2±0.7	7±1.4
sinusoidal cells		0.4±0.1	0.4±0.1	6±1.8
Wilson's disease, liver biopsy				
hepatocytes				
cytosolic granules[b]	patient 1	7±1	50±4	28±3
	patient 2	6±1	17±2	48±5
	patient 3	6±1	9±2	24±3
nuclei	patient 1	8±1	40±6	40±6
	patient 2	6±1	15±2	43±6
	patient 3	6±1	10±2	23±3
sinusoidal cells				
	patient 1	40±13	200±59	101±21
	patient 2	6±2	19±9	40±4
	patient 3	7±3	10±4	21±5
LEC rats, liver				
hepatocytes				
cytosol	rat 1	6±1.2	19±3.8	26±4.2
	rat 2	11±2	288±28	24±3
nuclei	rat 1	18±2.3	109±14	74.8±5.2
	rat 2	40±5.2	120±31	80±8.8
sinusoidal cells	rat 1	19±10	65±24	53±9
	rat 2	11±2.0	302±49	37±6.4

[a] This patient was found to be a heterozygote for Wilson's disease. Normal liver copper concentration is 9–27 $\mu g\,g^{-1}$ dry tissue (Scheinberg & Sternlieb 1984). Liver copper concentration in the patients with Wilson's disease was between 751 and 929 $\mu g\,g^{-1}$ dry tissue. In the absence of copper microprobe standards, relative concentrations as demonstrated by relative mass spectral peak intensity are the only comparisons we may make between Wilson's disease and control specimens.

[b] 'Granules': single membrane bound organelles, probably secondary lysosomes by TEM, appearing as dense bodies different from mitochondria when examined at ×1000 by the optical microscope of the LAMMA instrument. Not all cells had resolvable 'granules' at this magnification.

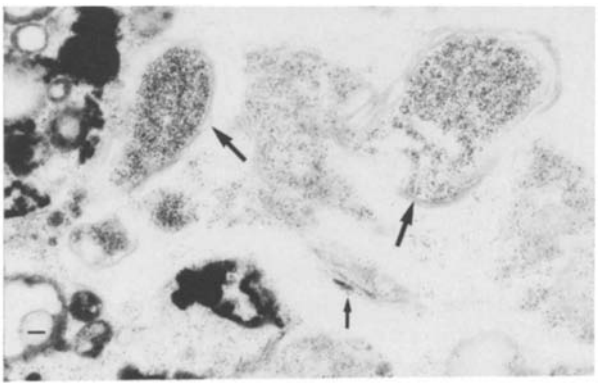

Figure 3. LEC rats show abnormal liver structure and ultrastructure. High magnification displays conspicuous ferritin in the cytosol and siderosomes (arrows) of sinusoidal cells, compatible with a haemolytic process in these icteric rats. Unstained. Bar: 100 nm.

Discussion

The purpose of the present study was to further investigate the use of LAMMA in a variety of pathological conditions, in view of the relatively few reports on its use with biological samples.

For the diagnosis of most cases of Gaucher disease, the morphologic, invasive investigation procedures are presently an anachronism (Beutler 1992). Nevertheless, the presence of iron in these cells, first revealed by Lorber (1960) deserved investigation. Additional studies confirmed this finding (Lee *et al.* 1967) and ferritin was identified as the iron-storing compound in Gaucher cells (Lorber & Nemes 1967). However, the relatively low magnifications used, and staining of ultrathin sections, did not allow for clear identification of typical ferritin particles and determination of their exact location within various subcellular compartments. The typical tubular structures of Gaucher bodies formed by

crystallization of glucocerebroside have flat layers as their fundamental morphologic unit and appear to develop by digestion of ingested erythrocytes (Naito *et al.* 1988). LAMMA examination of numerous Gaucher cells showed a clear difference between the low iron content of the glucocerebroside-containing tubular structures and the remainder of Gaucher cell cytoplasm with a high iron-related signal. Electron microscopy further identified the nature of this uneven distribution, with conspicuous ferritin and haemosiderin in the cytoplasm, and only extremely rare ferritin particles in the tubular bodies. Assembly of holoferritin molecules from apoferritin and the iron derived from phagocytized erythrocytes would be expected to be localized in the Gaucher cell cytosol, and not within the typical twisted multilayers or flat layers of crystallized glucocerebroside. The absence of excess iron in cultured skin fibroblasts of patients with Gaucher disease favours the concept of the extrinsic origin (erythrophagocytosis) of the iron found in typical Gaucher cells. In addition, the negative findings in cultured fibroblasts suggest that cells without apparent involvement in the pathologic process may not express significant changes in trace element content. Preliminary LAMMA and TEM studies of cultured fibroblasts from patients with Niemann Pick, Krabbe and Tay–Sachs diseases, sialidosis, and neuronal ceroid lipofuscinosis, sustain this view (Iancu *et al.*, unpublished observations).

Samples from spontaneous or experimentally induced iron overload generated spectra with extremely high iron-related peaks. In general, the identification by laser microprobe analysis of the cell population with the highest iron peaks confirmed the concept of an initial predominant channelling of excess iron depending on its origin. Under this concept, nutritional-enteric iron is channelled to parenchymal cells while transfusional-parenteral iron is channelled to RES cells. Thus, LAMMA confirmed the preponderant hepatic parenchymal cell overload in neonatal haemochromatosis, genetic haemochromatosis and pretransfusional thalassaemia major, where iron arises from nutritional/maternal sources. The major role of the RES pathway in the storage of injected iron is illustrated by the baboon (Table 2). Despite a massive RES siderosis and redistribution of iron to hepatocytes, this experimentally treated primate developed only transient elevation of aminotransferases and no cirrhosis (Brissot *et al.* 1983, Iancu *et al.* 1985). The extremely high iron peaks obtained when a dense siderosome (i.e. 'haemosiderin granule' by Perls' stain) is probed, demonstrate the efficiency of the lysosomal compartment in binding very large amounts of otherwise toxic iron. Cells containing numerous siderosomes continue to function normally for variable periods of time. It has been proposed that the formation of haemosiderin represents a biological protective mechanism, in that it decreases the ability of iron to promote oxygen radical reactions (O'Connell *et al.* 1986). According to the LAMMA data, the amount of iron segregated in the siderosomes is exceedingly large: the mass 56 peaks appearing in the LAMMA spectra are saturated and although intense do not reflect the total amount of such an abundant component of these structures. The iron-related peaks detected in nuclei of many hepatocytes and sinusoidal cells can be related to ferritin particles, which were identified in the nuclei of cells with conspicuous overload. The origin of nuclear ferritin is still unclear, but the size of the nuclear pore could allow for retrograde movement of ferritin particles from the cytosol.

A finding of the LAMMA study which deserves attention is the presence of aluminium ($m/z = 27$) in spectra obtained from siderosomes. In cases of iron overload, the aluminium-related peaks were especially high when the iron-related peak was prominent (Figure 1d and Table 2). The association between iron overload and increased aluminium toxicity has been noted in a variety of situations (Martin 1986, Good *et al.* 1992a,b). In the mechanism of iron toxicity, this association is especially significant at the molecular level, with ferritin involved not only in iron binding, but in binding aluminium as well (Dedman *et al.* 1992, Fleming & Joshi 1991). Moreover, aluminium has been found to enhance iron-induced lipid peroxidation (Gutteridge *et al.* 1985). The origin of aluminium identified in siderosomes by LAMMA is unclear, especially since it is found when no obvious exogenous source of aluminium can be identified (e.g. neonatal haemochromatosis and the pretransfusional stage of thalassaemia major). However, it is believed to be transported by transferrin-mediated mechanisms (Roskams & Connor 1990). The presence of prominent aluminium peaks in siderosome-derived spectra is suggestive of accumulation of ferritin-bound aluminium in these organelles, similarly to the siderosomic segregation of iron-containing ferritin.

In addition to the demonstration of a parallel siderosomic accumulation of aluminium and iron, the present study also provided information on possible trace element interactions. In recent years, attention has been focused mainly on the practical significance of antagonist interactions between two nutrients, in which one ion decreases the bioavailability of another. This is exemplified best by the zinc–copper antagonism, in which excess zinc markedly reduces the bioavailability of copper. Conversely, an example of synergistic metal ion interaction is that of copper and iron, in as much as copper is essential for iron absorption and metabolism. The multiple interactions of zinc, copper and iron, and their bioavailability, have been examined mainly from the nutritional physiologic point of view (O'Dell 1989). At the cellular level, LAMMA confirmed earlier studies showing that, at least in ruminant animals, excess iron interacts negatively with copper (O'Dell 1985). Increasing Fe:Cu ratios reduced the hepatic storage of copper in pigs (Hedges & Kornegay 1973) and in guinea pigs (Smith & Bidlack 1980). This was especially noticeable in the LAMMA spectra from compartments with extremely prominent iron peaks (i.e. siderosomes), which showed very low copper-related signals (Table 2). The fact that a negative copper–iron interaction was not observed by LAMMA in conditions with abnormal copper metabolism, such as Wilson's disease and the LEC rat, may derive from the lesser iron overload as well as the more diffuse distribution of copper in various subcellular compartments, including cell sap and nuclei, in these conditions.

The present study, the first by LAMMA of abnormal copper metabolism, has confirmed the presence of copper in hepatocytes as well as in sinusoidal and other RES cells, in Wilson's disease patients and LEC rats. Detection of copper in nuclei was surprising and suggests there may be a physiological as well as pathological role of copper there. Patient 3 had advanced Wilson's disease with liver failure and coagulation disturbances, and his liver biopsy was postponed until 2 months after initiation of penicillamine therapy. The low mass 63 signal in this patient may be a result either of therapy or of the end-stage liver disease. Copper-related signal intensities in LEC rats were of similar magnitude to those derived from Wilson's disease, except for the nuclei of hepatocytes of LEC rats in which the signal was much higher than in those of Wilson's disease. This likely resulted from the disease process itself since human and animal samples were handled and prepared in a similar manner.

Striking iron-related peaks were obtained from probing sinusoidal cells of Wilson's disease patient 1 who had also haemolytic anaemia and had been treated with transfusions, as well as in sinusoidal cells of LEC rats (Table 3). TEM of LEC rats confirmed that these iron signals originated in conspicuous ferritin and haemosiderin seen in reticuloendothelial cells (Figure 3 and Table 4), probably as a result of haemolysis. Yano *et al.* (1991) studied hepatic copper and iron in LEC rats and Wilson's disease by energy dispersive X-ray microanalysis of unstained ultrathin sections. In their report, copper-rich hepatocellular lysosomes were rare, and lysosomal copper content was low in both pre- and posticteric rats. Lysosomal iron was found frequently in Kupffer cells of posticteric rats as well as in a patient in convalescence, supporting the view that the RES iron is related to the haemolytic process. In a recent histochemical study of LEC rats, Sumi *et al.* (1993) found that the intense staining for copper and iron was limited to Kupffer cells in the liver, and no staining was seen in hepatocytes. This is apparently due to the intense binding of copper by metallothionein and illustrates only one of the confounding factors in the interpretation of histochemical stainings.

In summary, the present study has shown that LAMMA technology is valuable for investigating the distribution and relative quantitation of iron, aluminium and copper at subcellular sites in biomedical specimens. In both humans and experimental models, LAMMA enables one to follow both the time course and location of the process of iron overload and the effect of therapeutic agents. Among abnormalities of copper metabolism, Menkes disease and infantile childhood cirrhosis are presently being investigated. Finally, the examination of organs others than the liver, especially the brain, will provide important, presently missing, information on the role of various elements in both physiologic and pathologic processes.

Acknowledgements

This work was supported in part by Grant CH93 from The Milman Fund for Pediatric Research to T.C.I., the Lusk Fund for Surgical and Medical Sciences to E.H.K., Grant DK 34668 from the NIDDKD to I.S., and Grants AG 5238 and ES-928 from NIH to D.P.P. Tissue specimens studied included liver samples from baboon, provided by Professor P. Brissot (Liver Unit, INSERM U49, Rennes, France), and hornbill, provided by Professor T. J. Peters and Dr R. J. Ward (Department of Clinical Biochemistry, King's College School of Medicine and Dentistry, London, UK).

References

Beutler E. 1992 Gaucher disease: new molecular approaches to diagnosis and treatment. *Science* **256,** 794–799.

Brissot P, Campion JP, Guillouzo A, *et al.* 1983 Experimental hepatic iron overload in the baboon: Results of a two-year study. *Dig Dis Sci* **28,** 616–624.

Dedman DJ, Treffry A, Candy JM, *et al.* 1992 Iron and aluminium in relation to brain ferritin in normal individuals and Alzheimer's disease and chronic renal-dialysis patients. *Biochem J* **297,** 509–514.

Fleming JT, Joshi JG. 1991 Ferritin: the role of aluminum in ferritin function. *Neurobiol Aging* **12,** 413–418.

Good PF, Perl DP, Bierer LM, Schmeidler J. 1992 Selective accumulation of aluminum and iron in the neurofibrillary tangles of Alzheimer's disease: a laser microprobe (LAMMA) study. *Ann Neurol* **31,** 286–292.

Good PF, Olanow CW, Perl DP. 1992 Neuromelanin-containing neurons of the substantia nigra accumulate iron and aluminum in Parkinson's disease: a LAMMA study. *Brain Res* **593,** 343–346.

Gutteridge JM, Quinlan GJ, Clark I, Halliwell B. 1985 Aluminum salts accelerate peroxidation of membrane lipids stimulated by iron salts. *Biochem Biophys Acta* **835,** 441–447.

Hedges JD, Kornegay ET. 1973 Interrelationship of dietary copper and iron as measured by blood parameters, tissue stores and feedlot performance of swine. *J Anim Sci,* **37,** 1147–1154

Hillenkamp F, Kaufmann R, Nitsche R, Remy E, Unsöld E. 1974 Recent results in the development of a laser microprobe. In: Hall T, Echlin P, Kaufmann R, eds. *Microprobe Analysis as Applied to Cells and Tissues.* New York: Academic Press; 1–14.

Iancu TC. 1983 Iron overload. *Mol Aspects Med* **6,** 1–100.

Iancu TC, Landing BH, Neustein HB. 1977 Pathogenetic mechanisms in hepatic cirrhosis of thalassemia major: light and electron microscopic studies. *Pathol Am* **12,** 171–200.

Iancu TC, Rabinowitz H, Brissot P, Guillouzo A, Deugnier Y, Bourel M. 1985 Iron overload of the liver in the baboon. An ultrastructural study. *J Hepatol* **1,** 261–275.

Iancu TC, Shiloh H, Raja KB, *et al.* 1995 The hypotransferrinaemic mouse: ultrastructural and laser microprobe analysis observations. *J Pathol* **177,** 83–94.

Knisely AS. 1992 Neonatal hemochromatosis. *Adv Pediatr* **39,** 383–403.

Lee RE, Balcerzak SP, Westerman MP. 1967 Gaucher's disease. A morphologic study and measurements of iron metabolism. *Am J Med* **42,** 891–898.

Lorber M. 1960 The occurrence of intracellular iron in Gaucher's disease. *Ann Intern Med* **53,** 293 305.

Lorber M, Nemes JL. 1967 Identification of ferritin in Gaucher cells. *Acta Haematol* **37,** 189–197.

Li Y, Togashi Y, Sato S, Emoto T, Kang J-H, Takeichi N. 1991 Spontaneous hepatic copper accumulation in Long-Evans cinnamon rats with hereditary hepatitis. A model of Wilson disease. *J Clin Invest* **87,** 1858–1861.

Martin BR. 1986 The chemistry of aluminum as related to biology and medicine. *Clin Chem* **32,** 1797–1806.

Naito M, Takahashi K, Hojo H. 1988 An ultrastructural and experimental study on the development of tubular structures in the lysosomes of Gaucher cells. *Lab Invest* **58,** 590–598.

O'Connell M, Halliwell H, Moorhouse CP, Aruoma OI, Baum H, Peters TJ. 1986 Formation of hydroxyl radicals in the presence of ferritin and hemosiderin. *Biochem J* **234,** 727–731.

O'Dell BL. 1985 Bioavailability of and interactions among trace elements. In: Chandra RK, ed. *Trace Elements in Nutrition of Children*, New York/Vevey: Nestle Nutrition, Raven Press 41–62.

Perl DP, Good PF. 1992 Comparative techniques for determining cellular iron distribution in brain tissues. *Ann Neurol* **32,** S76–S81.

Roskams AJ, Connor JR. 1990 Aluminum access to the brain: a role for transferrin and its receptor. *Proc Natl Acad Sci USA* **87,** 9024–9027.

Scheinberg HI, Sternlieb I. 1984 *Wilson's Disease*. Philadelphia: WB Saunders.

Schmidt PF, Fromme HG, Pfefferkorn G. 1980 LAMMA investigations of biological and medical specimens. *Scanning Electron Microsc* **II,** 623–634.

Simpson RJ, Lombard M, Raja KR, Thatcher R, Peters TJ. 1991 Iron absorption by hypotransferrinaemic mice. *Br J Haematol* **78,** 565–570.

Simpson RJ, Konijn AM, Lombard M, Raja KB, Salisbury JR, Peters TJ. 1993 Tissue iron loading and histopathological changes in hypotransferrinemic mice. *J Pathol* **171,** 237–244.

Smith CH, Bidlack WR. 1980 Interrelationships of dietary ascorbic acid and iron on the tissue distribution of ascorbic acid, iron and copper in female guinea pigs, *J Nutr* **110,** 1398–1408.

Sumi Y, Kawahara S, Kikuchi Y, Sawada JI, Suzuki T, Suzuki TK. 1993 Histochemical and immunohistochemical localization of copper, iron and metallothionein in the liver and kidney of LEC rats. *Acta Histochem Cytochem* **26,** 5–9.

Verbeuken AH, Bruynseels FJ, Van Grieken R, Adams F. Laser microprobe mass spectrometry. In: Adams F, Gijbels R, Van Grieken R, eds. *Organic Mass Spectrometry*. New York: Wiley; 173–256.

Ward RJ, Iancu TC, Henderson GM, Kirkwood JR, Peters TJ. 1988 Hepatic iron overload in birds: analytical and morphological studies. *Avian Pathol* **17,** 451–464.

Wu J, Forbes JR, Chen HS, Cox DW. 1994 The LEC rat has a deletion in the copper transporting ATPase gene homologous to the Wilson disease gene. *Nature Genet* **7,** 541–545.

Yano M, Nishimura N, Takigawa T, *et al.* 1991 Hepatic copper and iron in LEC rats and patients with Wilson's disease. *J Clin Electr Microsc* **24,** 608 (abstr.).